An Infrared Spectroscopic and Theoretical Study of Group 4 Transition Metal $CH_2{=}MCl_2$ and $HC{\div}MCl_3$ Complexes

Jonathan T. Lyon and Lester Andrews*

Department of Chemistry, University of Virginia, P.O Box 400319, Charlottesville, Virginia 22904-4319

Received September 13, 2006

Laser-ablated group 4 transition metal atoms react with CH_2Cl_2 and $CHCl_3$ to yield the singlet $CH_2{=}MCl_2$ and triplet $HC{\div}MCl_3$ complexes, respectively. These products are identified by infrared spectra, isotopic substitution of the reactant precursors, and comparison to density functional theoretically predicted vibrational modes for the lowest energy structures. The computed $CH_2{=}MCl_2$ methylidene structures show no evidence of agostic distortion, in contrast to the previously investigated $CH_2{=}MHCl$ complexes. In the triplet $HC{\div}MCl_3$ complexes, the two unpaired electrons on carbon interact with the transition metal center and contribute weak π bonding. Comparisons with the analogous fluorinated complexes are given.

1. Introduction

Metal−carbon bonds are fundamentally important, and the entire organometallic subset of chemistry is devoted to them. Double-bonded alkylidene complexes in particular are of considerable interest for their roles in catalysis, and early transition metal alkylidenes have been proposed as reaction intermediates.[1−3] Carbon−halogen bond activation is also of considerable interest as a possible means of remediation for chlorofluorocarbons.[4−7]

Recently our group has investigated the reactions of group 4 transition metals with CH_4 and CH_3X molecules.[8−16] In these studies, the primary reaction products are double-bonded methylidene complexes, which show considerable agostic interactions between the metal center and the bonded C−H electrons. Methylene fluoride reacted with titanium to form the $CH_2{=}TiF_2$ methylidene complex.[17] However, in this instance no agostic distortion was observed. Fluorine lone pair repulsions were suggested to prevent this novel interaction. Recently, theoretical calculations have predicted that agostic bonds have strengths similar to weak hydrogen bonds.[18] In addition, titanium reacted with fluoroform to produce the analogous $CHF{=}TiF_2$ methylidene, which exhibited no distortion, but zirconium and hafnium formed the more stable triplet $HC{\div}MF_3$ complexes.[19] In these novel complexes the two unpaired electrons on carbon are shared with the electron-deficient metal center to give additional π bonding. We now report on the reaction products formed between group 4 transition metals and the chlorinated analogues (CH_2Cl_2 and $CHCl_3$) for comparison.

The goals of this study are as follows. In the reactions with dichloromethane, we wish to investigate whether $CH_2{=}MCl_2$ methylidenes form similarly to the fluorine analogues, or if chlorine substitution alters the reaction pathway. The C−Cl bonds are easier to break than C−F bonds, but the bulkier chlorine atoms are also slower to transfer, and H transfer might compete. Recall that H transfer produced the $CH_2{=}TiHCl$ complex from the Ti + CH_3Cl reaction.[16] If the $CH_2{=}MCl_2$ complexes are formed, will the complex be symmetrical like $CH_2{=}TiF_2$ or distorted like $CH_2{=}TiHCl$? As the group 4 transition metals gave different products in the reaction with CHF_3, we now wish to investigate how the chlorine analogues alter this reaction pathway and to compare the resulting products with those formed in fluoroform reactions.

2. Experimental and Theoretical Methods

Our experimental methods have been described in detail elsewhere.[20,21] In brief, laser-ablated transition metal atoms, generated by a Nd:YAG laser (1064 nm), were co-deposited with reagent gas diluted in argon (0.4−1.0%) onto a CsI window cooled to 8 K for the duration of 1 h. Infrared spectra were collected at 0.5 cm^{-1} resolution in the 400−4000 cm^{-1} region on the matrix-isolated reaction products by a Nicolet Magna 550 spectrometer with a HgCdTe type B detector at 77 K. Matrixes were subjected to UV irradiation for 10 min periods using a medium-pressure mercury arc lamp (Philips, 175 W) with the globe removed ($\lambda > 220$ nm) and annealings to various temperatures. Infrared spectra were collected after each procedure.

* Corresponding author. E-mail: lsa@virginia.edu.

(1) Schrock, R. R. *Chem. Rev.* **2002**, *102*, 145.
(2) Wada, K.; Pamplin, C. B.; Legzdins, P.; Patrick, B. O.; Tsyba, I.; Bau, R. *J. Am. Chem. Soc.* **2003**, *125*, 7035.
(3) Bailey, B. C.; Fan, H.; Baum, E. W.; Huffman, J. C.; Baik, M.-H.; Mindiola, D. J. *J. Am. Chem. Soc.* **2005**, *127*, 16016.
(4) Burdeniuc, J.; Jedlicka, B.; Crabtree, R. H. *Chem. Ber./Recl.* **1997**, *130*, 145.
(5) Yang, H.; Gao, H.; Angelici, R. J. *Organometallics* **1999**, *18*, 2285.
(6) Kraft, B. M.; Lachicotte, R. J.; Jones, W. D. *J. Am. Chem. Soc.* **2001**, *123*, 10973.
(7) Scott, V. J.; Celenligil-Cetin, R.; Ozerov, O. V. *J. Am. Chem. Soc.* **2005**, *127*, 2852.
(8) Andrews, L.; Cho, H.-G. *Organometallics* **2006**, *25*, 4040.
(9) Andrews, L.; Cho, H.-G.; Wang, X. *Inorg. Chem.* **2005**, *44*, 4834 (Ti+CH_4).
(10) Cho, H.-G.; Wang, X.; Andrews, L. *J. Am. Chem. Soc.* **2005**, *127*, 465 (Zr+CH_4).
(11) Cho, H.-G.; Wang, X.; Andrews, L. *Organometallics* **2005**, *24*, 2854 (Hf+CH_4).
(12) Cho, H.-G.; Andrews, L. *Inorg. Chem.* **2004**, *43*, 5253 (Ti+CH_3F).
(13) Cho, H.-G.; Andrews, L. *J. Phys. Chem. A* **2004**, *108*, 6294 (Ti+CH_3F).
(14) Cho, H.-G.; Andrews, L. *J. Am. Chem. Soc.* **2004**, *126*, 10485 (Zr+CH_3F).
(15) Cho, H.-G.; Andrews, L. *Organometallics* **2004**, *23*, 4357 (Hf+CH_3F).
(16) Cho, H.-G.; Andrews, L. *Inorg. Chem.* **2005**, *44*, 979 (Ti+CH_3Cl).
(17) Lyon, J. T.; Andrews, L. *Organometallics* **2006**, *25*, 1341 (Ti+CH_2F_2).
(18) von Frantzius, G.; Streubel, R.; Brandhorst, K.; Grunenberg, J. *Organometallics* **2006**, *25*, 118.
(19) Lyon, J. T.; Andrews, L. *Inorg. Chem.*, in press [IC061701L] (Ti, Zr, Hf+CH_2F_2 and CHF_3).
(20) Andrews, L. *Chem. Soc. Rev.* **2004**, *33*, 123.
(21) Wang, X.; Andrews, L. *Phys. Chem. Chem. Phys.* **2005**, *7*, 3834.

10.1021/om0608399 CCC: $37.00
Publication on Web 12/15/2006

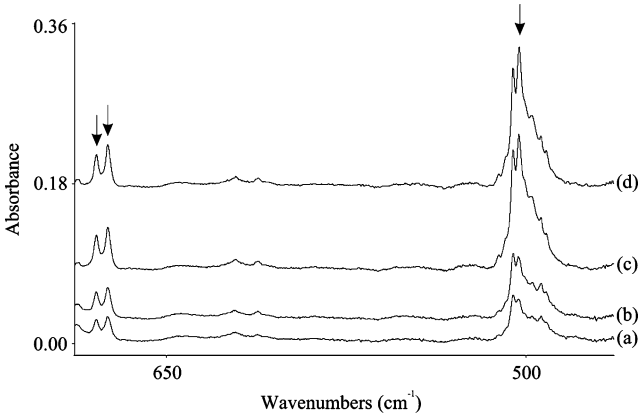

Figure 1. Infrared spectra taken in the 690−460 cm^{-1} region after (a) laser-ablated titanium atoms were reacted with CH_2Cl_2/Ar, and the resulting matrix was subjected to (b) irradiation with $\lambda > 290$ nm, (c) irradiation with $\lambda > 220$ nm, and (d) annealing to 30 K. Arrows denote product absorptions.

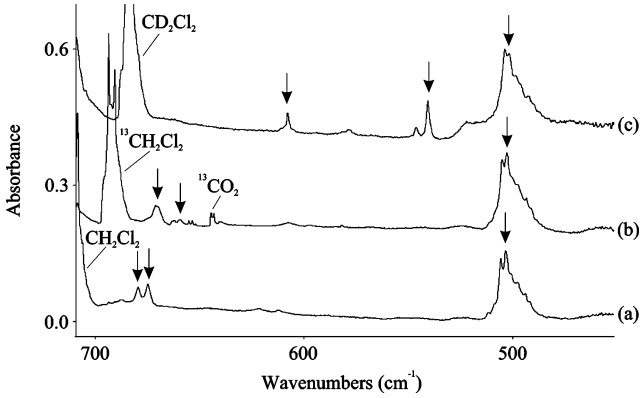

Figure 2. IR spectra taken in the 710−450 cm^{-1} region taken after laser-ablated titanium atoms were reacted with (a) CH_2Cl_2, (b) $^{13}CH_2Cl_2$, and (c) CD_2Cl_2 diluted in argon. All spectra were recorded after full-arc photolysis ($\lambda > 220$ nm). Arrows denote product absorptions.

Unless otherwise noted, all theoretical calculations were computed using the Gaussian '98 package.[22] The B3LYP hybrid functional[23] was used with the 6-311++G(2d,p) basis for all atoms except the transition metal, where the SDD pseudopotential was employed.[24,25] These calculations will enable comparisons with other methylidene complexes.[8−19] Vibrational frequencies were computed analytically, and all energy values reported include zero-point vibrational corrections. As a calibration, our calculation for the stable molecule $TiCl_4$ gave a tetrahedral structure with a strong IR mode at 499.7 cm^{-1}, which compares favorably with the argon matrix absorption[26a] at 502.6 cm^{-1}. Our DFT calculation predicts $TiCl_4$ to be more stable than Ti and two Cl_2 by 285 kcal/mol, which may be compared to the gas phase thermodynamic value of 295 ± 2 kcal/mol.[26b]

3. Results and Discussion

Reactions between group 4 transition metals and CH_2Cl_2 or $CHCl_3$ will be investigated, and product infrared spectra and DFT calculations will be reported in turn.

3.1. Ti + CH_2Cl_2. When laser-ablated titanium atoms react with methylene chloride, new product absorptions are observed at 503.0 with matrix site splitting at 505.5, 675.0, and 679.7 cm^{-1}. All three absorptions increase in unison on all photolysis, remain nearly unchanged on annealing (Figure 1), and maintain constant relative intensity in experiments with different precursor concentrations. (Arrows are used to denote product absorptions in all figures.) Hence the three observed bands can be assigned to a single reaction product. The strongest absorption, at 504.3 cm^{-1}, remains nearly unchanged on ^{13}C and D isotopic substitution (0.5 and 1.9 cm^{-1} shifts, respectively). This is also only slightly higher than the 502.6 cm^{-1} Ti−Cl stretching mode in $TiCl_4$.[26a] Hence, the observed product absorption can be assigned to a Ti−Cl stretching frequency. The next highest peak, at 675.0 cm^{-1}, shows a modest 5.3 cm^{-1} carbon-13 shift and a large 134.5 cm^{-1} deuterium isotopic shift (frequency ratio 1.249) (Figure 2). These values are similar to those for the observed CH_2 wagging motion of the CH_2═TiF_2 complex (695.4 cm^{-1}; 6.0 and 138.6 cm^{-1} ^{13}C and D shifts, respectively).[17] The last observed vibration at 679.7 cm^{-1} shows the largest carbon-13 shift (20.1 cm^{-1}) and a modest deuterium shift (71.9 cm^{-1}), and it can be assigned to a mostly C═Ti stretching mode. A final fourth absorption was observed at 978.9 cm^{-1} only in experiments when CD_2Cl_2 was employed.

The three identified product modes (Ti−Cl stretch, CH_2 wag, and C═Ti stretch) lead to identification of the stable CH_2═$TiCl_2$ complex with confidence. Our computed frequencies for this complex compare favorably with the observed spectrum (Table 1). Typically DFT-computed frequencies are a few percent higher than observed values.[9−16,26c] The fourth strongest mode predicted for the CH_2═$TiCl_2$ complex (Ti−Cl symmetric stretch; 374.7 cm^{-1}) is below our spectral limits. The CH_2 bending mode was computed to be nearly twice as intense for the deuterated isotopomer at 1033.1 cm^{-1} and is in satisfactory agreement with the fourth peak observed at 978.9 cm^{-1} when CD_2Cl_2 was employed. This gain in intensity is due to increased coupling with the C═Ti stretching mode.

Singlet methylidene CH_2═$TiCl_2$ is predicted to be 127 kcal/mol more stable than the sum of the individual methylene chloride and titanium atom reactants and 29 kcal/mol more stable than the triplet $CH_2(\mu$-Cl)TiCl primary insertion product. Another possible singlet methylidene complex, CHCl═TiHCl, is 62 kcal/mol higher in energy than CH_2═$TiCl_2$, and the computed vibrational spectrum is vastly different (including a strong Ti−H stretching mode near 1700 cm^{-1}, which is not observed). Although α-H transfer may be faster than α-Cl transfer, the latter is much more favorable energetically. The CH_2═$TiCl_2$ complex has been studied theoretically over the last two decades;[27−37] however, this is the first experimental observation to our knowledge.

(22) Frisch, M. J.; Trucks, G. W.; Schlegel, H. B.; Scuseria, G. E.; Robb, M. A.; Cheeseman, J. R.; Zakrzewski, V. G.; Montgomery, J. A., Jr.; Stratmann, R. E.; Burant, J. C.; Dapprich, S.; Millam, J. M.; Daniels, A. D.; Kudin, K. N.; Strain, M. C.; Farkas, O.; Tomasi, J.; Barone, V.; Cossi, M.; Cammi, R.; Mennucci, B.; Pomelli C.,; Adamo, C.; Clifford, S.; Ochterski, J.; Petersson, G. A.; Ayala, P. Y.; Cui, Q.; Morokuma, K.; Rega, N.; Salvador, P.; Dannenberg, J. J.; Malick, D. K.; Rabuck, A. D.; Raghavachari, K.; Foresman, J. B.; Cioslowski, J.; J. V. Ortiz,; Baboul, A. G.; Stefanov, B. B.; Liu, G.; Liashenko, A.; Piskorz, P.; Komaromi, I.; Gomperts, R.; Martin, R. L.; Fox, D. J.; Keith, T.; Al-Laham, M. A.; Peng, C. Y.; Nanayakkara, A.; Challacombe, M.; Gill, P. M. W.; Johnson, B.; Chen, W.; Wong, M. W.; Andres, J. L.; Gonzalez, C.; Head-Gordon, M.; Replogle, E. S.; Pople, J. A. *Gaussian 98*, Revision A.11.4; Gaussian, Inc.: Pittsburgh, PA, 2002.

(23) (a) Becke, A. D. *J. Chem. Phys.* **1993**, *98*, 5648. (b) Lee, C.; Yang, Y.; Parr, R. G. *Phys. Rev. B* **1988**, *37*, 785.

(24) Frisch, M. J.; Pople, J.A.; Binkley, J.S. *J. Chem. Phys.* **1984**, *80*, 3265.

(25) Andrae, D.; Haeussermann, U. Dolg, M.; Stoll, H.; Preuss, H. *Theor. Chim. Acta* **1990**, *77*, 123.

(26) (a) Königer, F.; Carter, R. O.; Müller, A. *Spectrochim. Acta* **1976**, *32A*, 891. (b) Cox, J. D.; Wagman, D. D.; Medvedev, V. A. *CODATA, Key Values for Thermodynamics*; Hemisphere Publishing Corp: New York, 1989. (c) Scott, A. P.; Radom, L. *J. Phys. Chem.* **1996**, *100*, 16502.

(27) Rappé, A. K.; Goddard, W. A. *J. Am. Chem. Soc.* **1982**, *104*, 297.

(28) Rappé, A. K.; Goddard, W. A. *J. Am. Chem. Soc.* **1982**, *104*, 448.

Table 1. Observed and Calculated Fundamental Frequencies of $CH_2{=}TiCl_2$[a]

approximate mode (symmetry)[b]	$CH_2{=}TiCl_2$		$^{13}CH_2{=}TiCl_2$		$CD_2{=}TiCl_2$	
	obs	calc (int)	obs	calc (int)	obs	calc (int)
HCTiCl dist (a′)		54.5 (27)		54.2 (27)		52.9 (26)
ClTiCl bend (a′)		108.4 (3)		108.1 (3)		107.7 (3)
CTiCl bend (a″)		171.2 (2)		168.8 (2)		141.2 (0)
CH_2 rock (a″)		273.7 (7)		270.7 (6)		232.6 (6)
Ti−Cl stretch (a′)		374.7 (32)		374.1 (32)		373.2 (31)
CH_2 twist (a″)		443.6 (0)		443.6 (0)		314.7 (0)
Ti−Cl stretch (a″)	503.0	523.4 (175)[c]	502.5	522.4 (176)	501.1	518.4 (177)
CH_2 wag (a′)	675.0	725.3 (122)[c]	669.7	718.5 (118)	540.5	572.9 (89)
C=Ti stretch (a′)	679.7	735.0 (41)[c]	659.6	718.9 (43)	607.8	654.2 (28)
CH_2 bend (a′)		1308.0 (18)		1298.2 (16)	978.9	1033.1 (28)
CH stretch (a′)		3056.5 (2)		3051.0 (2)		2215.9 (4)
CH stretch (a″)		3151.8 (2)		3139.6 (2)		2339.0 (1)

[a] B3LYP//6-311++G(2d,p)/SDD level of theory. All frequencies are in cm^{-1}, and computed infrared intensities are in km/mol. [b]Mode symmetries for C_s molecule. [c]B3LYP/6-311++G(3df,3pd) calculated frequencies (intensities) are 517.8 (171), 730.9 (112), and 725.4 cm^{-1} (48), respectively.

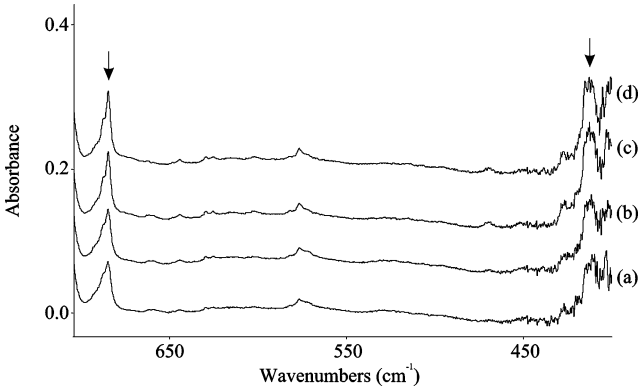

Figure 3. Infrared spectra taken in the 700−400 cm^{-1} region after (a) laser-ablated zirconium atoms were reacted with CH_2Cl_2/Ar, and the resulting matrix was subjected to (b) irradiation with $\lambda > 290$ nm, (c) irradiation with $\lambda > 220$ nm, and (d) annealing to 30 K.

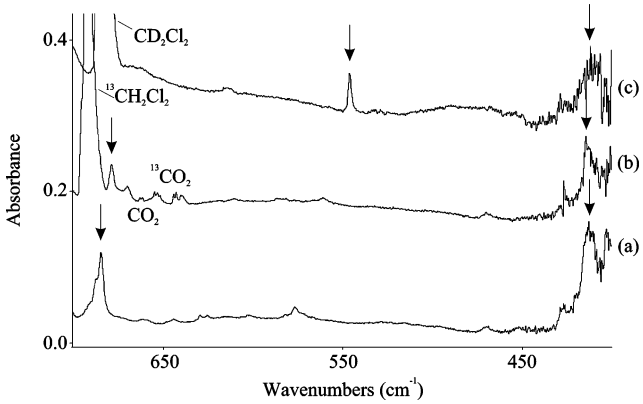

Figure 4. IR spectra taken in the 700−400 cm^{-1} region taken after laser-ablated zirconium atoms were reacted with (a) CH_2Cl_2, (b) $^{13}CH_2Cl_2$, and (c) CD_2Cl_2 diluted in argon. All spectra were recorded after full-arc photolysis ($\lambda > 220$ nm).

3.2. Zr + CH_2Cl_2. Zirconium atoms react with dichloromethane to form a single reaction product with infrared absorptions at 412.7 and 685.1 cm^{-1}. These absorptions increase slightly on photolysis and remain nearly unchanged on annealing (Figure 3). The 685.1 cm^{-1} absorption shows a modest 5.8 cm^{-1} ^{13}C isotopic shift and a large 139.0 cm^{-1} deuterium isotopic shift, as shown from comparison of spectra using $CHCl_3$, $^{13}CHCl_3$, and $CDCl_3$ in Figure 4. This peak is only 10.1 cm^{-1} higher than the CH_2 wagging mode of the $CH_2{=}TiCl_2$ complex, and it has a comparable 1.255 H/D isotopic frequency ratio. The vibration at 412.7 cm^{-1} is just above our spectral limit. It shows almost no carbon and hydrogen isotopic dependency (0.1 and 1.5 cm^{-1} ^{13}C and D shifts, respectively) and can be assigned to a Zr−Cl stretching mode. This absorption is only slightly below that observed for $ZrCl_4$.[38]

The identification of these modes (Zr−Cl stretch and CH_2 wag) indicate the observed product is $CH_2{=}ZrCl_2$. A comparison of our observed and theoretically predicted vibrations is given in Table 2. Again, the DFT-computed frequencies are slightly higher than observed values, and the CH_2 wag, which has considerable anharmonicity based on the H/D frequency ratio, is predicted least accurately by the harmonic frequency calculation. Notice that the CD_2 scissoring mode, which was observed only when titanium was reacted with CD_2Cl_2, was not observed for the zirconium analogue, as it is predicted to fall underneath the precursor absorption. Finally, $CH_2{=}ZrCl_2$ is computed to be 163 kcal/mol lower in energy than the sum of the zirconium atom and methylene chloride precursors.

3.3. Hf + CH_2Cl_2. Dichloromethane reacts with hafnium atoms to yield a single product with one strong infrared absorption at 677.6 cm^{-1}. This absorption shifts 6.0 cm^{-1} on ^{13}C isotopic substitution and shows a large 131.3 cm^{-1} deuterium isotopic shift (H/D frequency ratio 1.240), which are characteristic of a CH_2 wagging mode.

The observed absorption matches that predicted for the strongest absorption of the $CH_2{=}HfCl_2$ complex (Table 3). As in the case with zirconium, the anharmonic CH_2 wagging mode is predicted about 10% too high, but the isotopic shifts are predicted extremely well for this complex. The two Hf−Cl stretching modes are expected to fall below our spectral limits (B3LYP predicts them at 349.1 and 395.9 cm^{-1}). Hence we assign the observed band to the $CH_2{=}HfCl_2$ methylidene. This complex is computed to be 157 kcal/mol lower in energy than the sum of the two individual reactants.

3.4. Ti + $CHCl_3$. The reaction between laser-ablated titanium atoms and $CHCl_3$ yielded a single product with two infrared absorptions at 498.3 and 700.4 cm^{-1} (Figure 5). The lower absorption at 498.3 cm^{-1} showed 0.3 and 2.0 cm^{-1} shifts upon

(29) Francl, M. M.; Pietro, W. J.; Hout, R. F.; Hehre, W. J. *Organometallics* **1983**, *2*, 281.
(30) Francl, M. M.; Pietro, W. J.; Hout, R. F.; Hehre, W. J. *Organometallics* **1983**, *2*, 815.
(31) Gregory, A. R.; Mintz, E. A. *J. Am. Chem. Soc.* **1985**, *107*, 2179.
(32) Dobbs, K. D.; Hehre, W. J. *J. Am. Chem. Soc.* **1986**, *108*, 4663.
(33) Rappé, A. K. *Organometallics* **1987**, *6*, 354.
(34) Cundari, T. R.; Gordon, M. S. *J. Am. Chem. Soc.* **1992**, *114*, 539.
(35) Yamasaki, T.; Goddard, W. A. *J. Phys. Chem. A* **1998**, *102*, 2919.
(36) Cundari, T. R.; Klinckman, T. R. *Inorg. Chem.* **1998**, *37*, 5399.
(37) Böhme, U.; Beckhaus, R. *J. Organomet. Chem.* **1999**, *585*, 179.
(38) (a) Büchler, A.; Berkowitz-Mattuck, J. B.; Dugre, D. H. *J. Chem. Phys.* **1961**, *34*, 2202. (b) Godnev, I. N.; Aleksandrovskaia, A. M.; Rigina, I. V. *Opt. Spectrosc.* **1959**, *7*, 172.

Table 2. Observed and Calculated Fundamental Frequencies of $CH_2{=}ZrCl_2$[a]

approximate mode (symmetry)[b]	$CH_2{=}ZrCl_2$		$^{13}CH_2{=}ZrCl_2$		$CD_2{=}ZrCl_2$	
	obs	calc (int)	obs	calc (int)	obs	calc (int)
HCZrCl dist (a′)		30.8 (30)		30.6 (29)		30.0 (28)
ClZrCl bend (a′)		92.7 (3)		92.5 (3)		92.1 (3)
CZrCl bend (a″)		126.7 (0)		125.6 (0)		99.0 (0)
CH_2 rock (a″)		249.8 (4)		245.6 (3)		224.0 (2)
Zr−Cl stretch (a′)		348.6 (29)		348.4 (29)		348.3 (29)
Zr−Cl stretch (a″)	412.7	426.4 (147)	412.6	425.3 (147)	411.2	421.7 (147)
CH_2 twist (a″)		470.0 (0)		470.0 (0)		333.1 (0)
C=Zr stretch (a′)		703.7 (59)		685.1 (58)		632.0 (44)
CH_2 wag (a′)	685.1	745.4 (132)	679.3	738.6 (128)	546.1	585.9 (97)
CH_2 bend (a′)		1318.6 (15)		1310.1 (13)	*c*	1023.5 (29)
CH stretch (a′)		3044.7 (0)		3039.0 (0)		2209.5 (3)
CH stretch (a″)		3127.2 (5)		3115.4 (5)		2318.4 (2)

[a] B3LYP//6-311++G(2d,p)/SDD level of theory. All frequencies are in cm^{-1}, and computed infrared intensities are in km/mol. [b]Mode symmetries for C_s molecule. [c]Peak hidden behind precursor absorptions.

Table 3. Observed and Calculated Fundamental Frequencies of $CH_2{=}HfCl_2$[a]

approximate mode (symmetry)[b]	$CH_2{=}HfCl_2$		$^{13}CH_2{=}HfCl_2$		$CD_2{=}HfCl_2$	
	obs	calc (int)	obs	calc (int)	obs	calc (int)
HCHfCl dist (a′)		43.2 (20)		42.7 (20)		41.3 (19)
ClHfCl bend (a′)		91.2 (3)		90.8 (3)		90.0 (3)
CHfCl bend (a″)		138.5 (0)		136.8 (0)		111.3 (0)
CH_2 rock (a″)		281.1 (7)		277.5 (6)		247.2 (2)
Hf−Cl stretch (a′)		349.1 (25)		349.1 (25)		349.0 (25)
Hf−Cl stretch (a″)		395.9 (105)		394.2 (105)		386.1 (108)
CH_2 twist (a″)		462.3 (0)		462.3 (0)		328.5 (0)
C=Hf stretch (a′)		699.2 (45)		678.7 (44)		630.1 (33)
CH_2 wag (a′)	677.6	747.1 (103)	671.6	740.3 (99)	546.3	587.8 (77)
CH_2 bend (a′)		1323.2 (12)		1315.5 (10)	*c*	1018.6 (23)
CH stretch (a′)		3053.2 (0)		3047.4 (0)		2216.3 (2)
CH stretch (a″)		3130.1 (5)		3118.3 (5)		2320.0 (1)

[a] B3LYP//6-311++G(2d,p)/SDD level of theory. All frequencies are in cm^{-1}, and computed infrared intensities are in km/mol. [b]Mode symmetries for C_s molecule. [c]Peak hidden behind precursor absorptions.

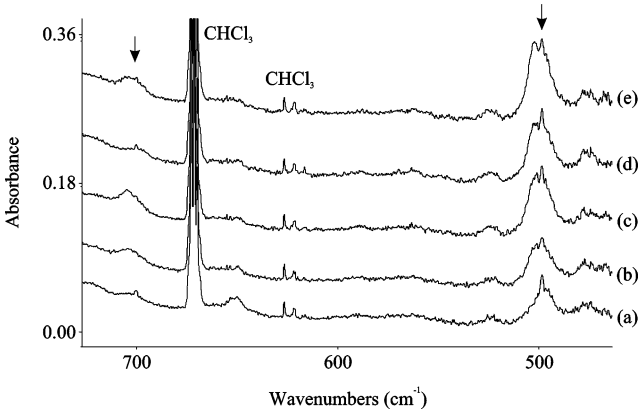

Figure 5. Infrared spectra taken in the 720−470 cm^{-1} region after (a) laser-ablated titanium atoms were reacted with $CHCl_3$/Ar, and the resulting matrix was subjected to (b) irradiation with $\lambda > 290$ nm, (c) irradiation with $\lambda > 220$ nm, (d) annealing to 30 K, and (e) a second irradiation with $\lambda > 220$ nm.

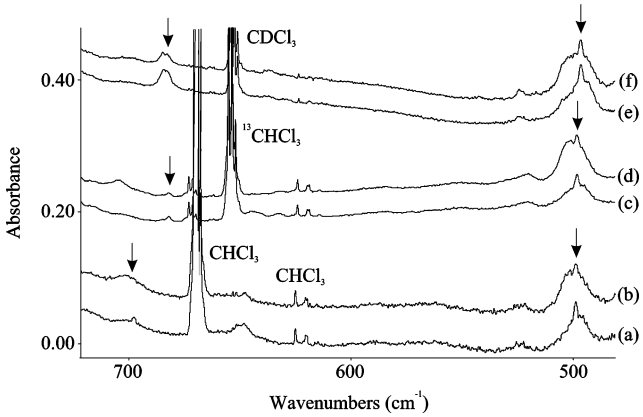

Figure 6. IR spectra taken in the 720−480 cm^{-1} region taken after laser-ablated titanium atoms were reacted with (a) $CHCl_3$, (c) $^{13}CHCl_3$, and (e) $CDCl_3$ diluted in argon, and (b, d, and f) after the resulting matrixes were subjected to full-arc photolysis ($\lambda > 220$ nm).

^{13}C and D isotopic substitution, respectively, indicating a Ti−Cl stretching mode, which is 4.7 cm^{-1} below this mode for $CH_2{=}TiCl_2$. The second absorption at 700.4 cm^{-1} shifted 18.3 cm^{-1} on carbon-13 substitution and 17.5 cm^{-1} on deuterium substitution (Figure 6) and must be assigned to a mostly carbon−titanium stretching mode.[39] Finally, the shoulder absorption near 503 cm^{-1} is probably due to $TiCl_4$.[26a]

Computations on the possible singlet $CHCl{=}TiCl_2$ complex led to a product 134 kcal/mol lower in energy than the sum of the individual reactants.[40] When titanium was reacted with CHF_3, the $CHF{=}TiF_2$ complex was the lone observed product.[19] However, for the $CHCl{=}TiCl_2$ complex, three strong infrared absorptions are predicted at 487.7 (147 km/mol), 532.6 (96 km/mol), and 624.2 cm^{-1} (77 km/mol, C−H wagging mode), which does not match the observed spectrum. Next we computed the singlet $HC{-}TiCl_3$ complex, which converged to a bridge-bonded $HC(\mu\text{-}Cl)TiCl_2$ complex that is about 1 kcal/mol higher

(39) The "mostly C=Ti" and "mostly C÷Ti" stretching modes in these two product molecules are not strictly comparable, as the former is mixed with the CH_2 bend and the latter carries H.

(40) Optimized $CHCl{=}TiCl_2$ structure: Ti−Cl: 2.222 and 2.219 Å, C=Ti: 1.869 Å, C−Cl: 1.738 Å, C−H 1.094 Å, ∠ClTiCl: 132.2°, ∠ClTiC: 111.7 and 116.0°, ∠ClCTi: 131.2°, ∠HCTi: 118.1°, ∠ClCH: 110.7°.

Table 4. Observed and Calculated Fundamental Frequencies of HC÷$TiCl_3$[a]

approximate mode (symmetry)[b]	HC÷$TiCl_3$		H^{13}C÷$TiCl_3$		DC÷$TiCl_3$	
	obs	calc (int)	obs	calc (int)	obs	calc (int)
ClTiCl bend (e)		113.7 (0)		113.5 (0)		113.3 (2)
$TiCl_3$ umbrella (a_1)		130.5 (3)		129.9 (3)		129.9 (3)
CTiCl bend (e)		147.8 (6)		145.1 (6)		134.6 (6)
Ti−Cl stretch (a_1)		393.4 (20)		392.7 (19)		392.7 (19)
HCTi def (e)[c]		431.6 (6)		428.1 (8)		345.4 (10)
Ti−Cl stretch (e)[c]	498.3	494.6 (330)	498.0	494.1 (328)	496.3	491.3 (296)
C−Ti stretch (a_1)	700.4	713.4 (62)	682.1	694.4 (61)	682.9	691.1 (59)
C−H stretch (a_1)		3169.1 (14)		3158.8 (13)		2337.5 (15)

[a] B3LYP//6-311++G(2d,p)/SDD level of theory. All frequencies are in cm^{-1}, and computed infrared intensities are in km/mol. [b]Mode symmetries for C_{3v} molecule. [c]Mixed modes.

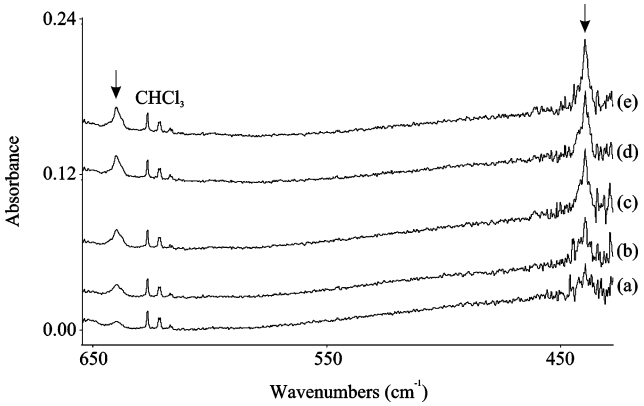

Figure 7. Infrared spectra taken in the 660−430 cm^{-1} region after (a) laser-ablated zirconium atoms were reacted with $CHCl_3$/Ar, and the resulting matrix was subjected to (b) irradiation with $\lambda > 290$ nm, (c) irradiation with $\lambda > 220$ nm, (d) annealing to 30 K, and (e) a second irradiation with $\lambda > 220$ nm.

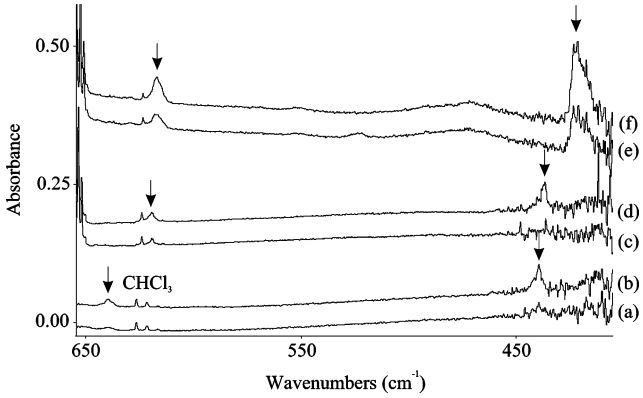

Figure 8. IR spectra taken in the 660−400 cm^{-1} region taken after laser-ablated zirconium atoms were reacted with (a) $CHCl_3$, (c) $^{13}CHCl_3$, and (e) $CDCl_3$ diluted in argon, and (b, d, and f) after the resulting matrixes were subjected to full-arc photolysis ($\lambda >$ 220 nm).

in energy than the CHCl═$TiCl_2$ methylidene. The triplet complex is 9 kcal/mol lower in energy than the bridged HC(μ-Cl)-$TiCl_2$ singlet species and 142 kcal/mol lower than the sum of the individual reactants. In related investigations, zirconium and hafnium metal atom reactions with CHF_3 formed triplet HC÷MF_3 complexes,[19] and the chlorinated analogues must be considered. Our theoretical computations predict the strongest infrared absorption (antisymmetric Ti−Cl stretch) of the triplet HC÷$TiCl_3$ complex to fall at 494.6 cm^{-1}, in good agreement with the observed Ti−Cl stretching mode at 498.3 cm^{-1} (Table 4). The second strongest mode (mostly C−Ti stretch) is predicted at 713.4 cm^{-1} with 19.0 cm^{-1} carbon-13 isotopic shift and 22.3 cm^{-1} D shift, which agrees well with the second observed product absorption (700.4 cm^{-1}; 18.3 cm^{-1} ^{13}C shift, 17.5 cm^{-1} D shift). The next strongest mode (Ti−Cl symmetric stretch) is predicted to fall below our spectral limits (393.4 cm^{-1}). Hence the two observed absorption peaks can be assigned to the triplet HC÷$TiCl_3$ complex.

3.5. Zr + $CHCl_3$. Laser-ablated zirconium atoms react with trichloromethane to yield infrared absorptions at 439.2 and 639.8 cm^{-1}. Both absorptions are characterized by the same behavior on photolysis and annealing and can be assigned to a single reaction product (Figure 7). The lower absorption at 439.2 cm^{-1} shows 2.6 and 16.8 cm^{-1} carbon-13 and deuterium isotopic shifts, respectively (Figure 8). This appears to be a predominantly Zr−Cl stretching mode, but must be mixed with another mode involving H(D). The upper absorption at 639.8 cm^{-1} shows a large 20.2 cm^{-1} ^{13}C isotopic shift and a 22.7 cm^{-1} D shift, which is appropriate for a strong mostly C−Zr stretching mode.

Computations on the possible singlet CHCl═$ZrCl_2$ methylidene complex converged to a structure lying 168 kcal/mol lower in energy than the sum of the initial reactants.[41] However, for this structure the two Zr−Cl stretching modes are predicted to be at or below our spectral limit (353.1 and 412.7 cm^{-1}), but the strongest observable absorption is predicted at 651.2 cm^{-1}, corresponding to the C−H wagging mode. No absorption was observed that showed a significant deuterium shift (the CHCl wagging mode of the CHCl═$ZrCl_2$ complex was predicted to show a 139.8 cm^{-1} shift upon D substitution). Next, the very stable triplet HC÷$ZrCl_3$ complex is 23 kcal/mol lower in energy than the methylidene species. For this complex, the mostly C−Zr stretching mode is predicted at 640.7 cm^{-1} with 19.9 and 22.6 cm^{-1} ^{13}C and D isotopic shifts, respectively (Table 5), which reproduce the observed absorptions with the expected accuracy. Our computations predict the Zr−Cl antisymmetric stretch (406.6 cm^{-1}) and the H−C−Zr deformation (449.9 cm^{-1}) modes to be highly mixed. The observed band at 439.2 cm^{-1} shows a 2.6 cm^{-1} ^{13}C isotopic shift, which agrees well with the predicted shift of the H−C−Zr deformation (3.3 cm^{-1}). However, the observed deuterated species absorption agrees better with the Zr−Cl stretching mode prediction as the D−C−Zr deformation shifts to lower frequency. Hence, the observed absorption is a mixture of the two modes, and the hydrogen counterpart is mostly H−C−Zr deformation and the deuterium counterpart mostly Zr−Cl antisymmetric stretch. The observed spectrum is assigned to the triplet HC÷$ZrCl_3$ complex, which is supported by comparison between calculated and observed frequencies in Table 5.

3.6. Hf + $CHCl_3$. Diluted chloroform in argon reacts with hafnium atoms to produce a single product with infrared

(41) Optimized CHCl═$ZrCl_2$ structure: Zr−Cl: 2.386 and 2.383 Å, C═Zr: 2.011 Å, C−Cl: 1.764 Å, C−H 1.093 Å, ∠ClZrCl: 130.9°, ∠ClZrC: 111.2 and 116.1°, ∠ClCZr: 127.3°, ∠HCZr: 122.8°, ∠ClCH: 109.8°.

Table 5. Observed and Calculated Fundamental Frequencies of HC÷$ZrCl_3$[a]

approximate mode (symmetry)[b]	HC÷$ZrCl_3$		H^{13}C÷$ZrCl_3$		DC÷$ZrCl_3$	
	obs	calc (int)	obs	calc (int)	obs	calc (int)
ClZrCl bend (e)		95.3 (1)		95.2 (1)		95.2 (1)
$ZrCl_3$ umbrella (a_1)		101.8 (6)		101.6 (6)		101.6 (6)
CZrCl bend (e)		132.9 (0)		130.0 (0)		122.8 (0)
Zr−Cl stretch (a_1)		367.6 (20)		367.4 (20)		367.4 (20)
Zr−Cl stretch (e)[c]		406.6 (71)		406.4 (68)	422.4	413.6 (131)
HCZr def (e)[c]	439.2	449.9 (79)	436.6	446.6 (81)		344.9 (5)
C−Zr stretch (a_1)	639.8	640.7 (75)	619.6[d]	620.8 (72)	617.1	618.1 (71)
C−H stretch (a_1)		3169.3 (5)		3159.1 (4)		2336.4 (9)

[a] B3LYP//6-311++G(2d,p)/SDD level of theory. All frequencies are in cm^{-1}, and computed infrared intensities are in km/mol. [b]Mode symmetries for C_{3v} molecule. [c]Mixed modes. [d]Peak mixed with weak precursor absorption.

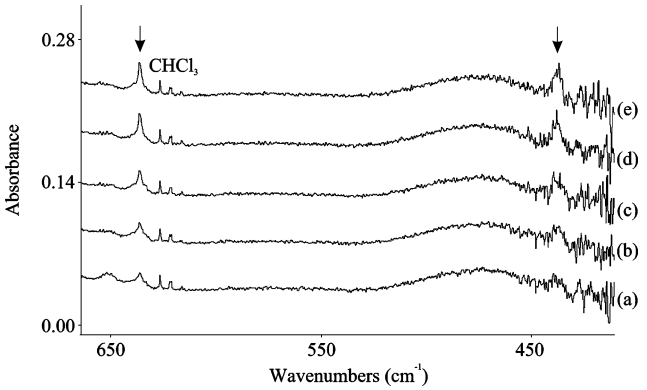

Figure 9. Infrared spectra taken in the 670−410 cm^{-1} region after (a) laser-ablated hafnium atoms were reacted with $CHCl_3$/Ar, and the resulting matrix was subjected to (b) irradiation with $\lambda > 290$ nm, (c) irradiation with $\lambda > 220$ nm, (d) annealing to 30 K, and (e) a second irradiation with $\lambda > 220$ nm.

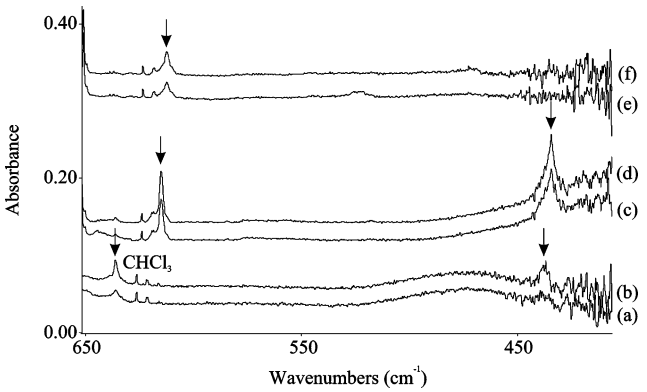

Figure 10. IR spectra taken in the 650−400 cm^{-1} region taken after laser-ablated hafnium atoms were reacted with (a) $CHCl_3$, (c) $^{13}CHCl_3$, and (e) $CDCl_3$ diluted in argon, and (b, d, and f) after the resulting matrixes were subjected to full-arc photolysis ($\lambda >$ 220 nm).

absorptions at 437.8 and 636.3 cm^{-1} (Figure 9). The upper absorption shows 21.2 and 23.8 cm^{-1} ^{13}C and D isotopic shifts, respectively, which is characteristic of a strong mostly C−Hf stretching mode. The second observed absorption at 437.8 cm^{-1} shows a 3.4 cm^{-1} carbon-13 isotopic shift (Figure 10).

The potential singlet methylidene CHCl═$HfCl_2$ is predicted to be 162 kcal/mol more stable than the sum of the reactants.[42] However, our computations on this complex predict the strongest infrared active mode within our spectral limits at 665.2 cm^{-1}, corresponding to the C−H wagging mode, which does not match our experimental results. Hence the product spectrum cannot be assigned to the CHCl═$HfCl_2$ species. However, once this complex is formed, the third chlorine atom can transfer to the hafnium metal center, which is predicted to be 4 kcal/mol lower in energy, conserving the singlet spin multiplicity, followed by spin relaxation to the triplet HC÷$HfCl_3$ complex, which is 32 kcal/mol lower in energy than the methylidene. The C−Hf stretching mode of this complex is predicted at 625.1 cm^{-1} with 20.9 and 23.6 cm^{-1} ^{13}C and D isotopic shifts, respectively, in excellent agreement with experiment (Table 6). The only other absorption predicted to be observed is the H−C−Hf deformation mode at 451.0 cm^{-1}, which is mixed with some Hf−Cl stretching character. A 3.4 cm^{-1} carbon-13 shift is computed for this absorption, in good agreement with the peak observed at 437.8 cm^{-1} showing a 3.4 cm^{-1} ^{13}C isotopic shift. This is an acetylenic-like C−H deformation mode. Hence, the observed vibrational spectrum is assigned to the triplet HC÷$HfCl_3$ complex.

3.7. Reaction Mechanisms. Following our investigations of the group 4 metal atom reactions with CH_4, CH_3X, and CH_2F_2 molecules,[8−17,19] these reactions with CH_2Cl_2 most likely proceed first through the triplet C−Cl insertion product.

$$M\ (^3F) + CH_2Cl_2 \rightarrow CH_2(\mu\text{-Cl})MCl\ (T) \quad (1a)$$

$$\rightarrow CH_2{-}MCl_2\ (T) \rightarrow CH_2{=}MCl_2\ (S) \quad (1b)$$

Alternative insertion into a C−H bond gives a higher energy $CHCl_2$−MH metal hydride product,[14] for which we find no evidence. Reaction 1a is predicted to be sufficiently exothermic (98, 91, and 102 kcal/mol lower in energy than the reactants for Ti, Zr, and Hf, respectively) to activate further α-Cl transfer rearrangement to the triplet CH_2−MCl_2 intermediate, which relaxes in the matrix to the lower energy singlet methylidene dichloride product (T and S denote triplet and singlet electronic states, respectively). The final Ti, Zr, and Hf methylidene dichloride products are 127, 163, and 157 kcal/mol, respectively, lower in energy than the precursors. Although α-H transfer might be faster, the alternative CHCl═TiHCl methylidene complex is 62 kcal/mol higher in energy and is not observed in these experiments.

The reaction with $CHCl_3$ begins in like fashion with C−Cl insertion.

$$M\ (^3F) + CHCl_3 \rightarrow CHCl(\mu\text{-Cl})MCl\ (T) \quad (2a)$$

$$\rightarrow CHCl{-}MCl_2\ (T) \rightarrow CHCl{=}MCl_2\ (S) \quad (2b)$$

$$\rightarrow HC{-}MCl_3\ (S) \rightarrow HC{\div}MCl_3\ (T) \quad (2c)$$

$$\rightarrow CHCl{-}MCl_2\ (T) \rightarrow HC{\div}MCl_3\ (T) \quad (2b')$$

(42) Optimized CHCl═$HfCl_2$ structure: Hf−Cl: 2.374 and 2.368 Å, C═Hf: 2.020 Å, C−Cl: 1.777 Å, C−H 1.090 Å, ∠ClHfCl: 125.6°, ∠ClHfC: 110.3 and 114.6°, ∠ClCHf: 123.0°, ∠HCHf: 127.3°, ∠ClCH: 109.5°.

Table 6. Observed and Calculated Fundamental Frequencies of HC÷HfCl$_3$[a]

approximate mode (symmetry)[b]	HC÷HfCl$_3$		H^{13}C÷HfCl$_3$		DC÷HfCl$_3$	
	obs	calc (int)	obs	calc (int)	obs	calc (int)
HfCl$_3$ umbrella (a_1)		92.8 (5)		92.7 (5)		92.7 (5)
ClHfCl bend (e)		93.3 (4)		93.3 (4)		93.3 (4)
CHfCl bend (e)		134.2 (0)		131.0 (0)		124.2 (0)
Hf−Cl stretch (a_1)		364.3 (18)		364.3 (18)		364.3 (18)
Hf−Cl stretch (e)[c]		375.7 (144)		375.7 (144)		378.4 (206)
HCHf def (e)[c]	437.8	451.0 (82)	434.4	447.6 (82)		348.1 (6)
C−Hf stretch (a_1)	636.3	625.1 (61)	615.1	604.2 (58)	612.5	601.5 (57)
C−H stretch (a_1)		3183.0 (5)		3172.8 (4)		2346.8 (9)

[a] B3LYP//6-311++G(2d,p)/SDD level of theory. All frequencies are in cm^{-1}, and computed infrared intensities are in km/mol. [b]Mode symmetries for C_{3v} molecule. [c]Mixed modes.

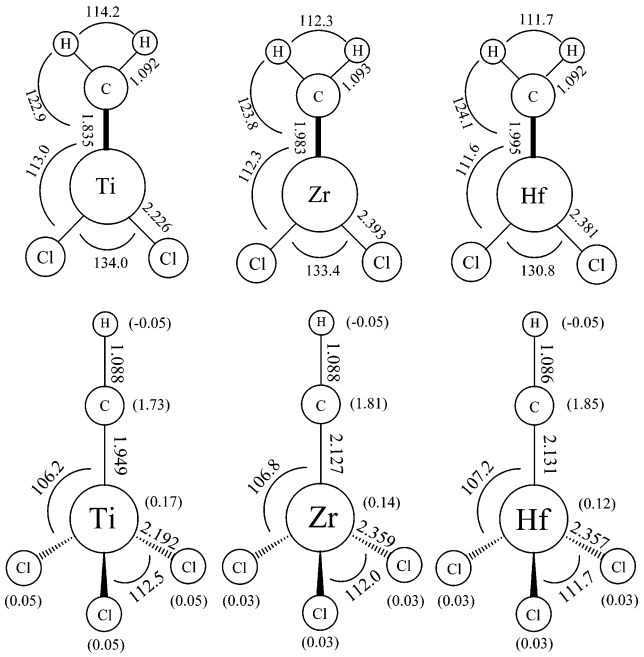

Figure 11. Optimized geometries (Å and deg) for the singlet $CH_2{=}MCl_2$ (C_s) and triplet HC÷MCl$_3$ (C_{3v}) complexes at the B3LYP//6-311++G(2d,p)/SDD level of theory. Atomic spin densities in parentheses are given by each atom in the triplet complexes.

The initial insertion product undergoes α-Cl transfer to form the triplet CHCl−MCl$_2$ species. Here, the reaction pathway can go one of two ways. First (reactions 2b and 2c), spin relaxation to the singlet CHCl=MCl$_2$ methylidene forms a stable species similar to the reactions with CH_2Cl_2. From here, the third α-Cl transfers to the metal center followed by spin relaxation to the very stable triplet HC÷MCl$_3$ complex. Alternatively, the HC÷MCl$_3$ complex could form directly via chlorine transfer in the triplet CHCl−MCl$_2$ complex (reaction 2b′), which is predicted to be only 2 kcal/mol higher in energy than the singlet CHCl=MCl$_2$ complex for titanium. Reactions with group 4 metals and CHF_3 follow the former reaction pathway, but C−Cl bonds are weaker than C−F bonds, and we cannot rule out the latter reaction pathway. Hence, we are unable to determine the reaction pathway from M + $CHCl_3$ to HC÷MCl$_3$ at this time.

3.8. Group Trends and Comparison to Fluorine Analogues. The geometries of the group 4 $CH_2{=}MCl_2$ complexes at the B3LYP level of theory are shown in Figure 11, and the structural parameters are summarized in Table 7. For comparison, a CCSD calculation of the $CH_2{=}TiCl_2$ complex with similar basis sets (SDD pseudopotential and 6-311++G(2d,2p)) was done using the NWChem Program.[43,44] This geometry[45] compares well with our B3LYP result and other computations reported for the $CH_2{=}TiCl_2$ complex,[27,29,30,32−34] although previous workers assumed a coplanar molecule. We find that the $CH_2{=}TiCl_2$ complex has one plane of symmetry (C_s) bisecting the Cl−Ti−Cl angle, and the Ti−Cl bonds are slightly out of the $CH_2{=}$Ti plane using the all-electron basis set for Ti. This nonplanarity increases for the Zr and Hf complexes. Hence we believe the B3LYP method is accurate for describing these complexes.

Table 7. Geometrical Parameters and Physical Constants of Ground State $CH_2{=}MCl_2$ (M = Ti, Zr, Hf)[a]

parameter	$CH_2{=}TiCl_2$[e]	$CH_2{=}ZrCl_2$	$CH_2{=}HfCl_2$
r(C−H)	1.092	1.093	1.092
r(C=M)	1.835	1.983	1.995
r(M−Cl)	2.226	2.393	2.381
∠(HCH)	114.2	112.3	111.7
∠(CMCl)	113.0	112.3	111.6
∠(ClMCl)	134.0	133.4	130.8
∠(HCM)	122.9	123.8	124.1
Φ(HCMCl)	0.0, 180.0	5.4, 171.7	9.0, 165.0
q(C)[b]	−0.56	−0.76	−0.77
q(H)[b]	0.15	0.13	0.09
q(M)[b]	0.81	1.37	1.62
q(Cl)[b]	−0.27	−0.43	−0.51
μ[c]	0.957	1.020	1.772
ΔE[d]	127	163	157

[a] Bond lengths and angles are in Å and deg. All calculations were performed at the B3LYP//6-311++G(2d,p)/SDD level. [b]Mulliken atomic charge. [c]Molecular dipole moment in D. [d]Binding energy in kcal/mol. [e]Dimensions for the B3LYP//6-311++G(2d,p) all-electron calculation are 1.092, 1.840, 2.234, 114.2, 113.7, 132.5, 122.9, 0.6, and 178.8, respectively.

It is of interest to reflect on the prevalence of agostic distortion in the simple group 4 methylidenes. The $CH_2{=}MH_2$ and $CH_2{=}$MHX complexes all possess agostic interactions.[9−16] However, it is important to note that the agostic bonds in the $CH_2{=}$MHX methylidenes are trans to the M−X bond. The $CH_2{=}MF_2$ and $CHF{=}MF_2$ complexes[17,19] (as well as the $CH_2{=}MCl_2$ species reported here) do *not* show any evidence of agostic interactions in the DFT-calculated structures. Clearly this is due to the presence of the second halogen atom on the metal center. One possible explanation is that halogen lone pair

(43) Scuseria, G. E.; Schaefer, H. F., III. *J. Chem. Phys.* **1989**, *90*, 3700, and references therein.

(44) Aprà, E.; Windus, T. L.; Straatsma, T. P.; Bylaska, E. J.; de Jong, W.; Hirata, S.; Valiev, M.; Hackler, M.; Pollack, L.; Kowalski, K.; Harrison, R.; Dupuis, M.; Smith, D. M. A; Nieplocha, J.; Tipparaju V.; Krishnan, M.; Auer, A. A.; Brown, E.; Cisneros, G.; Fann, G.; Früchtl, H.; Garza, J.; Hirao, K.; Kendall, R.; Nichols, J.; Tsemekhman, K.; Wolinski, K.; Anchell, J.; Bernholdt, D.; Borowski, P.; Clark, T.; Clerc, D.; Dachsel, H.; Deegan, M.; Dyall, K.; Elwood, D.; Glendening, E.; Gutowski, M.; Hess, A.; Jaffe, J.; Johnson, B.; Ju, J.; Kobayashi, R.; Kutteh, R.; Lin, Z.; Littlefield, R.; Long, X.; Meng, B.; Nakajima, T.; Niu, S.; Rosing, M.; Sandrone, G.; Stave, M.; Taylor, H.; Thomas, G.; van Lenthe, J.; Wong, A.; Zhang, Z. *NWChem*, A Computational Chemistry Package for Parallel Computers, Version 4.6; Pacific Northwest National Laboratory: Richland, WA, 2004.

(45) Optimized $CH_2{=}TiCl_2$ structure at CCSD//6-311++G(2d,2p)/SDD: Ti−Cl: 2.232 Å, C=Ti: 1.869 Å, C−H 1.088 Å, ∠ClTiCl: 135.8°, ∠ClTiC: 112.1°, ∠HCTi: 123.9°, ∠HCH: 112.3°.

Table 8. Geometrical Parameters and Physical Constants of Ground State $HC{\div}MCl_3$ (M = Ti, Zr, Hf)[a]

parameter	$HC{\div}TiCl_3$[e]	$HC{\div}ZrCl_3$	$HC{\div}HfCl_3$
r(C−H)	1.088	1.088	1.086
r(C÷M)	1.949	2.127	2.131
r(M−Cl)	2.192	2.359	2.357
∠(CMCl)	106.2	106.8	107.2
∠(ClMCl)	112.5	112.0	111.7
q(C)[b]	−0.28	−0.42	−0.39
q(H)[b]	0.18	0.16	0.21
q(M)[b]	0.71	1.27	1.31
q(Cl)[b]	−0.20	−0.34	−0.38
μ[c]	2.214	1.970	1.872
ΔE[d]	142	191	194
$\langle s^2 \rangle$	2.0104	2.0081	2.0076

[a] Bond lengths and angles are in Å and deg. All calculations were performed at the B3LYP//6-311++G(2d,p)/SDD level on the triplet $HC{\div}MCl_3$ species in C_{3v} symmetry. [b]Mulliken atomic charge. [c]Molecular dipole moment in D. [d]Binding energy in kcal/mol. [e]Dimensions for the B3LYP//6-311++G(3df,3pd) all-electron calculation are 1.087, 1.955, 2.199, 106.1, and 112.7, respectively.

repulsions are significantly strong to prohibit agostic distortion. This would also explain why the agostic bonds[18] in the $CH_2{=}MHX$ complexes are trans to the M−X bond. We note here that the C═Ti bond is 0.015 Å shorter in the $CH_2{=}TiCl_2$ than in the $CH_2{=}TiF_2$ complex, where fluorine lone pairs have been suggested to prevent agostic distortion.[17]

Also, as the group 4 metal atom gets heavier, the Cl−M−Cl and H−C−H angles both decrease, and the Cl atoms are more out of the $CH_2{=}M$ plane. However, they are all larger angles than found for the fluorine analogues.[19] Similar to the fluorine analogues, the HCMCl dihedral angles deviate more from 0°/180° moving down the group 4 transition series (Table 7), a trend discussed in more detail.[19] The $CH_2{=}MCl_2$ complexes are lower in energy than the individual reactants by 127, 163, and 157 kcal/mol for Ti, Zr, and Hf, respectively (Table 7). This is the same order observed for the fluorine analogues, but the $CH_2{=}MCl_2$ molecules are slightly less stable.[19] As the metal atom becomes larger, it is easier for the chlorine atoms to withdraw electron density from the metal atom. Hence, the Mulliken charges on the chlorine atoms become more negative, while the charges on the metal centers become more positive.

The $CH_2{=}MF_2$ and $CH_2{=}MCl_2$ complexes are symmetrical and isostructural. The C═M bond lengths are 0.015, 0.015, and 0.013 Å longer in the group 4 difluoride series, respectively.[17,19] The stronger inductive effect of fluorine relative to chlorine appears to weaken slightly the C═M bond. The CH_2 wagging modes in the $CH_2{=}MCl_2$ complexes discussed here are 20, 14, and 30 cm^{-1} lower than their $CH_2{=}MF_2$ counterpart values,[19] and they exhibit comparable anharmonicities (observed H/D isotopic frequency ratios 1.249, 1.255, 1.240, respectively, in the dichloride series). In contrast the harmonic frequency ratios calculated here for the mode are 1.266, 1.272, and 1.271, respectively.

We find one difference in structural preference for group 4 metal reaction products with CHF_3 and $CHCl_3$. In the case of Ti the products trapped are the methylidene $CHF{=}TiF_2$ and the electron-deficient methylidyne $HC{\div}MCl_3$, respectively. In the cases of Zr and Hf, both haloforms form the latter complex. Finally, we find no evidence for any higher energy α-H transfer products in these di- and trihalomethane systems.

For the three triplet state $HC{\div}MCl_3$ complexes, the Cl−M−Cl angles again become smaller with increasing metal size (Figure 11 and Table 8). It appears that halogen substitution for hydrogen in these complexes strengthens the C÷M bond. The C÷Ti bond length in $HC{\div}TiCl_3$ is only 0.003 Å longer than in the $ClC{\div}TiCl_3$ species,[46] indicating a similar bond strength in the two electron-deficient methylidyne complexes. However, the computed C÷Zr and C÷Hf bond lengths are 0.029 and 0.024 Å shorter in the trichloride than in the trifluoride species. The $HC{\div}MCl_3$ complexes are well-defined triplet species ($\langle s^2 \rangle$ values near 2.0, Table 8). The atomic spin densities total 2.00 (Figure 11) and show carbon 2p electron sharing with the metal center, which decreases with metal size as the C(2p)−M(nd) overlap decreases. Hence, two weak degenerate π bonds are formed to augment the single C−M bond in these electron-deficient methylidyne systems. This additional π bonding appears to be greater in the $ClC{\div}TiCl_3$ complex because of contribution from the single chlorine. The spin densities of Cl (0.22), C (1.29), Ti (0.34), and 3Cl (0.05) suggest a stronger π interaction in the latter complex.[46]

4. Conclusions

Laser-ablated group 4 transition metals react with CH_2Cl_2 and $CHCl_3$ to form $CH_2{=}MCl_2$ and $HC{\div}MCl_3$ complexes, respectively, which are trapped in solid argon. The $CH_2{=}MCl_2$ methylidenes show no agostic distortions and have slightly shorter computed carbon═metal bonds than the fluorine analogues. The triplet $HC{\div}MCl_3$ complexes have C_{3v} molecular symmetry. The two lone electrons on carbon are partially donated to the electron-deficient metal center, forming electron-deficient methyldyne complexes, and this π bonding interaction decreases with increasing metal size.

Acknowledgment is made to the Donors of the American Chemical Society Petroleum Research Fund for support of this research. This research was performed in part using the Molecular Science Computing Facility (MSCF) in the William R. Wiley Environmental Molecular Sciences Laboratory, a national scientific user facility sponsored by the U.S. Department of Energy's Office of Biological and Environmental Research and located at the Pacific Northwest National Laboratory. Pacific Northwest is operated for the Department of Energy by Battelle.

OM0608399

(46) The $ClC{\div}TiCl_3$ structure was optimized at the same theoretical level as that employed here (Cl−C: 1.630 Å, C÷Ti: 1.946 Å, Ti−Cl: 2.198 Å, ∠CTiCl: 106.3°, ∠ClTiCl: 112.4°).